Biochimica et Biophysica Acta 1853 (2015) 1596–1605

Contents lists available at ScienceDirect

Biochimica et Biophysica Acta

journal homepage: www.elsevier.com/locate/bbamcr

Iron for proliferation of cell lines and hematopoietic progenitors: Nailing down the intracellular functional iron concentration

Emmanuel Pourcelot [a,b,d,f], Marine Lénon [a,b], Nicolas Mobilia [f], Jean-Yves Cahn [e,f], Josiane Arnaud [a,b,g], Eric Fanchon [f], Jean-Marc Moulis [a,b,c,*], Pascal Mossuz [d,f]

[a] Université Grenoble Alpes, Laboratory of Fundamental and Applied Bioenergetics, and Environmental and Systems Biology, Grenoble, France
[b] Inserm, U1055, Grenoble, France
[c] Commissariat à l'Energie Atomique et aux Energies Alternatives–Institut de Recherches en Technologies et Sciences du Vivant, Grenoble, France
[d] CHU Grenoble, Laboratoire d'Hématologie, Institut de Biologie et Pathologie, Grenoble, France
[e] CHU Grenoble, Clinique d'hématologie, Grenoble, France
[f] Université Grenoble Alpes, TIMC–Imag CNRS 5525 Grenoble, France
[g] CHU Grenoble, Département de Biochimie, Toxicologie et Pharmacologie, Grenoble, France

ARTICLE INFO

Article history:
Received 13 January 2015
Received in revised form 25 February 2015
Accepted 19 March 2015
Available online 27 March 2015

Keywords:
Iron homeostasis
Post-transcriptional regulation
Leukemia
Cellular growth
Cell cycle
Modeling

ABSTRACT

Iron is an essential nutrient which must be provided in sufficient amounts to support growth of eukaryotic cells. All organisms devote specialized pathways to ensure proper delivery. Yet, a quantitative assessment of the intra-cellular iron concentration needed to allow the cell cycle to proceed in mammalian cells is missing. Starting from iron-depleted cell lines or primary hematopoietic progenitors prepared with clinically implemented iron chelators, replenishment via transferrin and other iron sources has been quantitatively monitored through the main endogenous markers of the cellular iron status, namely proteins involved in the uptake (transferrin receptor), the storage (ferritin), and the sensing (Iron Regulatory Proteins) of iron. When correlated with measurements of iron concentrations and indicators of growth, this minimally intrusive approach provided an unprecedented estimate of the intracellular iron concentration acting upon iron-centered regulatory pathways. The data were analyzed with the help of a previously developed theoretical treatment of cellular iron regulation. The minimal cellular iron concentration required for cell division was named *functional iron concentration* (FIC) to distinguish it from previous estimates of the cellular labile iron. The FIC falls in the low nanomolar range for all studied cells, including hematopoietic progenitors. These data shed new light on basic aspects of cellular iron homeostasis by demonstrating that sensing and regulation of iron occur well below the concentrations requiring storage or becoming noxious in pathological conditions. The quantitative assessment provided here is relevant for monitoring treatments of conditions in which iron provision must be controlled to avoid unwanted cellular proliferation.

1. Introduction

Iron is required to maintain viability and to support growth of almost all kinds of cells. In eukaryotes, it is abundantly present in the electron-transfer centers of the mitochondrial respiratory chain, for instance, and, more generally, it participates at the active sites of a myriad of proteins and enzymes. Consequently, iron is mandatory for cellular proliferation [1], and iron removal from the growth medium generally stops the cell cycle at the G1/S transition. One contributing factor to this blockade is the iron-dependent enzyme ribonucleotide reductase, which relies on a subunit containing a tyrosyl-di-iron cofactor [2]. The arrest of the cell cycle induced by iron chelators justifies considering these compounds as anti-neoplastic agents [3].

In metazoans, the most iron demanding pathway is erythropoiesis since iron is the anchoring site of oxygen in hemoglobin, a protein supplying oxygen to tissues. Iron-deficient individuals suffer from anemia,

Abbreviations: AML, acute myeloid leukemia; BSA, bovine serum albumin; DPF, deferiprone (3-hydroxy-1,2-dimethyl-4-pyridinone); DFO, deferoxamine; ESA, erythropoietic stimulating agents; EDTA, ethylene-diamine tetracetate; FAC, ferric ammonium citrate; FIC, functional iron concentration; HO-1, inducible heme oxygenase; IRP, Iron Regulatory Proteins; LIP, labile iron pool; MDS, myelodysplastic syndrome; NDRG1, N-myc downstream regulated 1; PBS, Phosphate buffered saline solution; PCBP, poly(rC) binding proteins; ROS, reactive oxygen species; Tf, transferrin

* Corresponding author at: LBFA-INSERM U1055, BP 53, F-38041 Grenoble Cedex 9 France. Tel.: +33 (0)4 76 63 55 36.
E-mail addresses: epourcelot@chu-grenoble.fr (E. Pourcelot), marine.lenon@ujf-grenoble.fr (M. Lénon), Nicolas.Mobilia@imag.fr (N. Mobilia), JYCahn@chu-grenoble.fr (J.-Y. Cahn), JArnaud@chu-grenoble.fr (J. Arnaud), Eric.Fanchon@imag.fr (E. Fanchon), jean-marc.moulis@cea.fr (J.-M. Moulis), PMossuz@chu-grenoble.fr (P. Mossuz).

http://dx.doi.org/10.1016/j.bbamcr.2015.03.009
0167-4889/

in which not enough iron is incorporated into nascent hemoglobin and which is the most widespread single nutrient deficiency worldwide [4,5]. Iron provision for hematopoiesis is delivered by transferrin (Tf), a circulating glycoprotein which can be easily measured together with its iron load to gauge the iron status. Although the critical levels of this useful biomarker have been set a long time ago, it remains unclear how much Tf-delivered iron is needed to support proliferation of cells that must divide to maintain homeostasis or to fulfill specific functions. Throughout hematopoiesis, cells must properly handle iron according to the specific requirements of the different stages, from renewal of stem cells to full differentiation of specialized blood components [6].

Cells need to maintain the proper level of iron availability, and this requirement is challenged in transfusion-induced iron overload or, conversely, by neoplasm-triggered large iron consumption. The former situation occurs in cases of thalassemia [7] and myelodysplastic syndromes [8], for instance. The latter applies to cancer cells in general, acute myeloid leukemia clones in particular, for which ample iron provision is needed to support growth, particularly in the blast crisis. The pivotal role of iron in such circumstances has recently been clearly evidenced by the redirection of proliferating blasts into the monocyte lineage with a treatment including iron chelation [9–11].

To clarify conditions under which cell proliferation occurs, the quantitative iron needs of model cell lines and of hematological progenitors for amplification have been evaluated herein. The implemented integrative approach minimally perturbed cells, and it allowed us to show that proliferation is supported by smaller amounts of iron than assumed before. With the help of a recently developed theoretical model of cellular iron homeostasis, these data should help understand the role of iron deregulation in a wealth of pathological conditions, and they will have to be considered for a better implementation of the therapeutic strategies targeting iron-dependent pathways.

2. Materials and methods

2.1. Reagents

All reagents were obtained from Sigma-Aldrich unless stated otherwise. Human holo-transferrin (i.e. iron-loaded transferrin, Sigma T4132) was iron saturated with 2 Fe atoms/molecule. The iron content of human apo-transferrin (apo-Tf), i.e. the protein devoid of iron, was measured by inductively coupled plasma-mass spectrometry at less than 0.025 iron atom/transferrin molecule. Recombinant human Iron Regulatory Proteins (IRP) 1 and 2 were obtained as previously detailed [12,13].

2.2. Cell lines

The cell lines used in the present study originated from the ATCC biological resource. The human myeloid leukemia KG1 and K562 cells were grown in RPMI-1640 medium, supplemented with 10% fetal bovine serum (Biowest, origin: South America, batch containing 1.7 mg of iron/l), 1% L-glutamine, 100 U of penicillin/ml and 0.1 mg steptomycin/ml at 37 °C with 5% CO_2. As a rapidly growing cell model significantly different from the above cell lines, HeLa cells were routinely maintained in Dulbecco's modified Eagle medium (DMEM) supplemented as above for leukemic cell lines. The iron-containing DMEM was replaced by RPMI after iron depletion for direct comparison of the iron-requirements of the HeLa cells as compared to the other cells used in this work.

2.3. Purification of $CD34^+$ progenitors

$CD34^+$ cells were obtained from cord blood after Ficoll-Hypaque (Abcys - Eurobio) density gradient separation and they were isolated by two steps of immunomagnetic separation (Miltenyi Biotec), on large then medium size columns, successively. Cord blood procedures were approved by the French Blood Service's Institutional Review Board, and samples were obtained from healthy donors who gave informed consent.

2.4. Iron depletion and proliferation assay for cell lines

After routine maintenance in rich media, cell lines were handled in a minimal medium composed of RPMI-1640, 1% treated (see below) bovine serum albumin (BSA), 30 nM sodium selenite, 1% L-glutamine, 100 U of penicillin/ml and 0.1 mg steptomycin/ml at 37 °C in 5% CO_2. In the case of HeLa cells, the minimal medium was used after adhesion in the conventional rich medium. To remove as much iron as possible, the BSA powder was dissolved in 10 mM HEPES buffer pH 7.3 containing 5 mM EDTA before dialysis with successive baths of distilled water until reaching an EDTA concentration below 1 nM. Beforehand, distilled water was filtered through Chelex cation exchange resin (BioRad). The BSA concentration was estimated by spectrophotometry at 280 nm ($\varepsilon = 39{,}600\ M^{-1}\ cm^{-1}$).

Cells were seeded at 5×10^5 cell/ml in minimal medium without added iron or Tf, and the chelating agent was added for 24 h. Deferoxamine mesylate salt was used at 200 μM and deferiprone at 500 μM. The depletion medium was replaced by the minimal medium supplemented with the wanted source of iron. Cells were further kept for 24 h, which is the optimum duration to measure growth at low iron concentrations before cell death, and the cells were then processed. Viable cells were determined by Trypan blue staining and quantified with a Luna™ counter (Logos).

2.5. Amplification, iron depletion, and proliferation assay for CD34 cells

A synthetic minimal medium was used to control iron supply. It was composed of Iscove's Modified Dulbecco's Medium (IMDM, Life Technologies), 1% iron-depleted albumin (as described above), 200 μg/ml insulin, 0.1 mM β-mercaptoethanol and the StemMACS HSC expansion cocktail (TPO/FLT3/SCF - Miltenyi Biotec) at 37 °C in 5% CO_2. Freshly isolated $CD34^+$ cells were seeded at 1×10^5 cells/ml and amplified for three days in the above minimal medium supplemented with 1.25 μM holo-Tf. Iron depletion and further experiments were carried out in the same medium in which the iron source was precisely monitored. Viable cells were determined by Trypan blue staining in Neubauer slides.

2.6. Cell cycle assays

Cells were rinsed and suspended at 3×10^6 cells/ml in Phosphate Buffered Saline (PBS) solution. They were fixed by slowly adding cold ethanol up to 50% (v:v) with thorough mixing. The suspension was left at 4 °C for one hour, the cells were centrifuged, washed with cold PBS, and suspended in PBS (4×10^6 cells/ml). RNA were degraded by 0.5 mg/ml RNAse A (Thermo Scientific) at 37 °C for 1 h, and cells were labeled by 10 μg/ml propidium iodide. The fluorescence was measured by flow cytometry with the LSR Fortessa™ cell analyzer (Becton Dickinson) using the 488 nm sapphire laser. The data were analyzed with the Modfit LT v3.2 software (Verity Software House).

2.7. Iron measurements

Iron concentrations were determined by Inductively Coupled Plasma-Mass Spectrometry (ICP-MS) using a XSERIES 2 analyzer (Thermo Scientific). Cellular pellets were suspended at 4000–8000 cells/μl of water. The volume corresponding to 8×10^5 cells was diluted (1:25) and mixed (1:1 v/v) with 1% nitric acid before analysis. Raw results were converted to cell associated concentrations by considering the estimated volumes of KG1 and K562 cells, 0.8 and 2.5 pL, respectively, in agreement with previously published values for the latter [14]. Gallium was used as internal

standard. For iron measurements in the growth media, 100 μl were directly treated with acid before analysis.

2.8. IRP activity measurement

IRP1 and IRP2 RNA-binding activities were measured by electrophoretic mobility shift assays with 3 μg of total protein extracts. The minimal sequence of human ferritin H-chain Iron Responsive Element (IRE) [12] was biotin-labeled with biotinylated cytidine (bis)phosphate using T4 RNA ligase (Thermo Scientific). The IRE-IRP reaction was carried out as previously described [12] and the complexes were separated on non-denaturing 4% PAGE in 0.5X TBE, transferred onto Hybond™ N^+ membrane (GE Healthcare) and the biotinylated bands were detected after interaction with the streptavidin-horseradish peroxidase conjugate by the chemiluminescent luminol product. Quantitation of the signals was done with the Image J software (v1.47, Wayne Rasband, Research Services Branch, National Institute of Mental Health, Bethesda, Maryland, USA).

2.9. Western blotting

Twenty to forty μg of total proteins were resolved by sodium dodecyl sulfate-polyacrylamide gel electrophoresis on 8% or 15% gels, and proteins were transferred to polyvinylidene difluoride membranes. For $CD34^+$ protein extracts, 8–16% gradient gels (Gene Bio-Application Ltd) were used. The blots were saturated with 10% non-fat milk in PBS-Tween 0.2% and probed overnight at 4 °C with antibodies (all produced in rabbit) against IRP1 (1:500) [15], ferritin (1:1000, Cell Signaling), heme oxygenase-1 (1:1000, Assay Designs), transferrin receptor 1 (1:1000, Abcam), and actin (1:250, Sigma Aldrich). Following three washes with PBS-Tween 0.2%, the blots were incubated with peroxidase-coupled goat anti-rabbit IgG (Bethyl) at a dilution of 1:5000 for 1 h at room temperature, followed by detection with the Pierce ECL western blotting substrate (Thermo Scientific).

2.10. Measurement of intracellular reactive oxygen species (ROS)

Intracellular ROS were measured using oxidant-sensitive fluorescent probes. Briefly, 500 000 cells were incubated without or with 200 μM carboxy-dichlorodihydrofluoresceinediacetate acetyl ester (carboxy-H_2DCFDA, Molecular Probes) and 10 μM dihydroethidium (DHE) at 37 °C in 5% CO_2 for 30 min. Then cells were washed in phosphate buffer saline before fluorescence measurement with the LSRFortessa™ FACS (Becton Dickinson) cytometer.

2.11. Measurement of lipid peroxidation

Cell pellets (7.5 10^5) were suspended in 0.4% (v:v) thiobarbituric acid, 50% acetic acid, 2 mM EDTA, and heated slightly below 100 °C for one hour. After cooling in ice the lysate was centrifuged for 10 min at 4000 *g*. The fluorescence of the supernatant (λ_{ex} = 535 nm; λ_{em} = 595 nm) was measured with the Infinite M200 plate reader (Tecan Group Ltd, Männedorf, Switzerland).

2.12. Measurements of mRNA

Total RNA was purified from KG1 and K562 cells grown in the absence and in the presence of 200 μM deferoxamine for 24 h. Complementary DNA was synthesized from 1 μg of RNA with modified Moloney Murine Leukemia virus reverse transcriptase (M-MuLV RT, Euromedex #09-11211) and oligo$(dT)_{12\text{-}18}$ primer, and diluted 30-fold. It was amplified by real-time qPCR (C1000 Thermal Cycler CFX96, BioRad), using validated primers and the HOT Pol Evagreen qPCR Mix Plus (Euromedex).

2.13. Statistical analysis

All quantitative variables were expressed as mean. Comparison of data was made using the Mann–Whitney *t*-test. Statistical analysis was performed using the STATVIEW® software package 5.0.

3. Results

3.1. Iron withdrawal and growth arrest

The myeloid leukemia cell lines used in this work are fast growing in a complete medium containing bovine serum with endogenous Tf. K562 and KG1 cells were treated with the clinically implemented iron chelator deferoxamine (DFO), with the aim of scavenging the essential metal nutrient in a relatively short time. Preliminary experiments showed that adding 200 μM DFO to cells growing in complete medium resulted in growth arrest within 24 h. The number of viable cells leveled off after treatment (Fig. 1A) with the disappearance of cells entering mitosis (Fig. 1B,C). Additional experiments using the same DFO concentration for a longer time, up to 72 h, indicated that cells progressively died. When the iron chelator had been added for 24 h, the residual intracellular iron concentration was unable to support growth. But actively growing cells divided for at least one generation when the complete medium without chelator was replaced by a minimal one devoid of iron-loaded Tf (see Section 2.4). As expected, the above observations are not restricted to the use of DFO, since a different iron-binding chemical, deferiprone (3-hydroxy-1,2-dimethyl-4-pyridinone, DPF), gave qualitatively similar results (Fig. 1).

The growth arrest induced by chelators was not paralleled by a significant increase of detectable oxidizing species in viable cells (Table S1). Accordingly, lipid peroxidation was not increased, and heme oxygenase 1 was not induced by the short term application of the chelators (Fig. S1). Overall, these results indicate that the iron-deprived viable cells do not experience significant oxidative stress.

3.2. Iron- or transferrin-triggered recovery from the iron-depleted state

Starting from the iron-depleted situation generated by the 24 h-treatment with 200 μM DFO, iron was added back to the medium without serum and the reversal of growth arrest was monitored by a series of complementary experiments. As can be seen in Fig. 2, and in agreement with former observations indicating that endocytosis of the Tf–Tf receptor complex is the privileged cellular iron uptake pathway [16], Tf was a far better mediator of iron provision to KG1 cells as compared to a simple iron salt such as ferric ammonium citrate (FAC). In these experiments, Tf is a key component of the medium since growth did not resume in the Tf-free minimal medium (Fe = 0 in Fig. 2). At least 10-times more iron provided by FAC was needed to increase the cell number in similar proportions to the situation in which iron is provided by loaded Tf. Yet, in both sets of conditions, viable cells efficiently recovered from the depleted situation without apparent harm and despite the absence of serum.

In the above experimental setting, the amount of Tf and associated iron needed to support growth can be precisely evaluated. Independent determinations in different experiments indicated that growth of K562 cells resumed after 24 h at Tf concentrations between 10 and 20 nM (Fig. 3A). The corresponding value for the KG1 cell line was shifted to below 5 nM fully loaded Tf (Fig. 2B). Accordingly, monitoring the cell cycle indicated that the proportion of G2/M cells progressively increased with the Tf concentration to reach a value similar to that displayed by actively growing cells in the presence of serum (Fig. 3A).

Considering the very low concentrations of Tf added to resume growth, it may be asked whether the effect is driven by added iron or is due to the Tf protein, a strong ferric iron binder of its own. To address

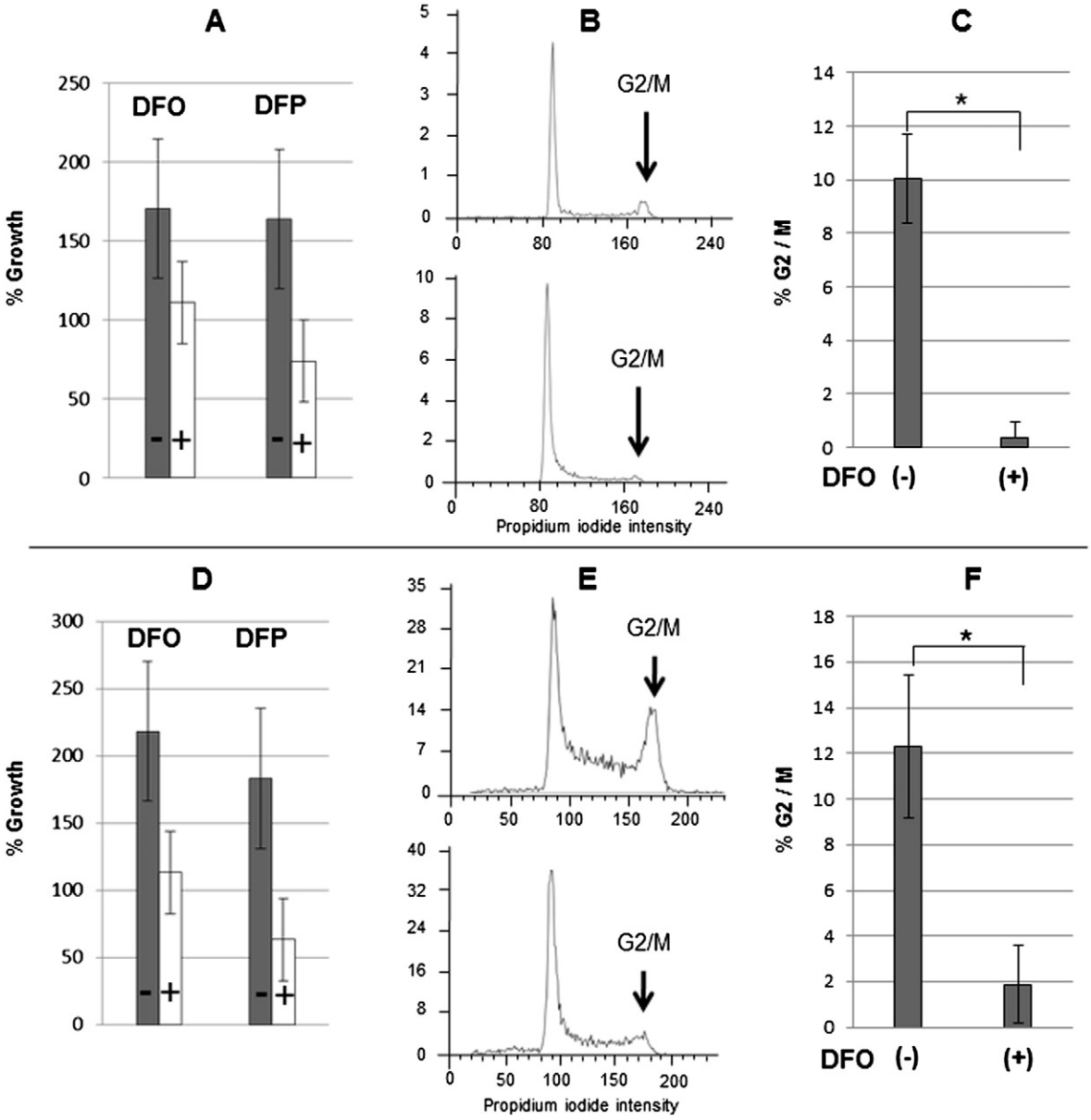

Fig. 1. Comparison of growing and chelator-treated cells. Top: KG1 cells. (A) The left panel shows the increase of viable cells (%) after 24 h in the conventional (serum-containing) growth medium (black bars) and after exposing them to either desferrioxamine (DFO, N = 6) or deferiprone (DFP) in the minimal medium devoid of serum (white bars). (B) Representative analysis of the cell cycle before (top) and after (bottom) application of DFO. (C) Percentage of mitotic cells under normal growth conditions (−) and after the DFO-treatment (+) (N = 4, * significant difference p = 0.0209). Bottom: Same experiments with the K562 cell line (D–F). The difference in the fraction of mitotic cells (F) is significant *, p = 0.0200 (N = 4).

this question apo-Tf (the iron-free protein), instead of holo-Tf (with bound iron), was used in the replenishment experiments. Apo-Tf concentrations as low as 15 nM were able to maintain viability of iron-depleted K562 cells for 24 h, and to reinitiate growth as witnessed by the re-appearance of the G2/M peak (Fig. 4). However, viability was not maintained under these conditions, i.e. without added loaded Tf, for more than 2 or 3 days. These experiments suggest that apo-Tf can mobilize some non-Tf bound iron brought by the medium or trapped by cells after treatment with the chelator. Yet, most of the non-Tf bound iron cannot be used by cells under these conditions, since viability and growth are supported for shorter duration than in the presence of holo-Tf.

The loss of cells in G2/M was also observed by treating HeLa cells with DFO. After iron depletion, viable cells re-entered the cell cycle (data not shown) as a function of the amount of re-added iron-loaded Tf at low concentrations (1–5 nM), in a range similar to that observed with KG1 cells (Fig. 2).

Thus the behavior of the cell lines upon iron recovery may quantitatively vary since growth of KG1 or HeLa cells resumed at smaller Tf concentrations than K562 cells. But the Tf concentration range rescuing growth arrest and death triggered by iron depletion and inducing re-entry into the cell cycle falls within a few tens of nM of Tf, at most, for all examined cell lines.

3.3. Molecular changes associated with iron replenishment

The iron concentration associated with cells followed the amount of added holo-Tf (Fig. 2; Fig. 3B). Yet, a consistent shift of the Tf concentration at which iron started to accumulate was observed (Fig. 2; Fig. 3A,B) compared to the concentrations triggering growth resumption, as monitored by increases in cell density and the development of the proportion of cells in the G2/M phase for instance. This indicates that iron storage occurs only when basic cellular needs are secured,

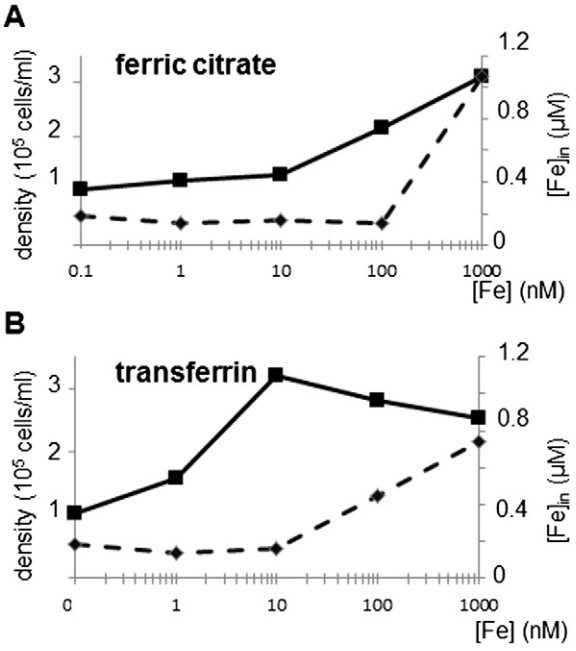

Fig. 2. Cell growth and intracellular iron replenishment of KG1 cells according to the iron source. Curves with black square marks represent the cell density after 24 h in minimal medium, starting from DFO-treated cells at 10^5 cells/ml. Dashed lines with cross marks represent calculated iron concentration associated with cells (see Section 2.7): the value measured without added iron (Fe = 0) corresponds to *ca.* 20 pmol Fe/10^6 KG1 cells. (A) Iron in the minimal growth medium provided by ferric ammonium citrate. (B) Same experiment with iron provided by holo-Tf.

including those required for proliferation in the present experimental conditions.

Ferritin is the protein responsible for intracellular iron storage. Immuno-detection of ferritin was found to follow the increase of intra-cellular iron as expected (Fig. 3B,D). In a mirroring function, the Tf receptor is all the more needed as iron is lacking. It thus decreased as more iron became available (Fig. 3C). Ferritin and Tf receptor 1 clearly increased and decreased, respectively, at lower Tf concentrations in KG1 cells (Fig. S2) than in K562 cells (Fig. 3).

The Iron Regulatory Proteins (IRP) were identified three decades ago as major regulators of ferritin and Tf receptor 1 translation [17,18]. According to its accepted mechanism, active IRP in iron limited conditions are repressors of ferritin translation and enhancers of Tf receptor 1 synthesis. In line with the results of the immuno-blots for ferritin and the Tf receptor 1, the IRP activity, but not the amount of the IRP1 protein, decreased as iron became available to cells via Tf (Fig. 3, Fig. S2). Changes in the concentration of other iron regulated proteins, such as NDRG1 (Fig. S3), were also observed in these experiments, which indicates that the implemented conditions largely dealt with iron/Tf effects rather than with less direct mechanisms. Indeed, lipid peroxidation, inducible heme oxygenase (HO-1), or oxidizing species concentrations did not significantly change in any of the samples (Table S1 and Fig. S1). Thus, the behavior of the studied cell lines cannot be explained by, or be associated with, iron mobilization by increased oxidative stress and cellular damage.

Apo-Tf can maintain viable iron-depleted cells for a short time (Fig. 4A) whereas cells without apo-Tf did not show any sign of growth (absence of G2/M cells for instance). However, addition of apo-Tf did not significantly change the IRP activity (Fig. 4B), the amount of the Tf receptor 1 (Fig. 4D), and only marginally ferritin (Fig. 4E). Also, the iron associated with cells did not dose-dependently follow added apo-Tf (Fig. 4C). Thus, whereas apo-Tf avoided immediate death of iron-depleted K562 cells, it did not display the dose dependency observed with holo-Tf (Fig. 3).

3.4. Derivation of the iron concentration needed for cellular growth

The data reported in Fig. 3 and S2 call for a quantitative assessment of the species under consideration. Toward this aim, it is convenient to use a previously developed theoretical framework [19] (and unpublished). The regulatory effect of iron on the IRP was represented by a sigmoid of the form $[Fe]^n/([Fe]^n + \theta^n)$, where [Fe] is the iron concentration detected by the regulatory system, θ is a value representing the iron threshold triggering the IRP activity (increasing below, disappearing above), and n is a number indicating the steepness of the sigmoid. Using this iron-dependency and assuming regulation by [Fe] has reached a stationary state at the time of the measurement, the variations of the IRP activity with [Fe] were adjusted according to:

$$IRP/IRP_{max} = ([Fe]^n + \theta^n)/((h+1)[Fe]^n + \theta^n) \quad (1)$$

Derivation of this equation is presented in Appendix A. IRP_{max} is the IRP activity measured without added Tf and considered to be maximal, and h is the ratio of the kinetic constants for the disappearance of IRP activity (the one in the presence of abundant iron divided by that in its absence). In the case of K562 cells the best adjustment of the data equating [Fe] in Eq. (1) to the provided Tf bound iron returned values of θ = 61.3 (SD 15.4) nM, h = 3.95 (SD 0.7), and n ~ 2 (Fig. 5). It means that the iron concentration modifying the IRP activity is that afforded by *ca.* 30 nM of added fully loaded Tf, and that the rate of disappearance of the IRP activity is 4-fold faster in the presence of iron than in its absence. A similar treatment of the data obtained with KG1 cells returned values close to 10 nM and 4 for θ and h, respectively (Fig. 5).

The values of h and n are similar in both cell lines (see also Table S2): this suggests that the mechanisms involved in regulating the IRP activity are conserved in different cells. The calculated values of θ deserve further analysis, because the correspondence between the added Tf-bound iron and the intracellular concentration detected by IRP is not straightforward. Fig. 3 shows that cell-associated iron started to increase at externally added Tf values higher than those triggering the decrease of IRP activity and the increase of the number of cells re-engaged in the cycle. This strongly suggests that all provided iron in the lowest Tf concentration range is readily used for biosynthetic needs without storage. Further, for a given cell type, a single set of parameters accounts for the sigmoidal dependence of IRP/IRP_{max} with [Fe] (Fig. 5). Thus, the amount of externally provided iron and the "IRP-detected" intracellular one are simply related and assumed to be proportional. But, since it is difficult to estimate the value of the proportionality coefficient from the data or from theoretical considerations, we let intracellular [Fe] of Eq. (1) vary between 1/100 and 100-fold the external Tf-bound iron concentration in adjustments similar to those of Fig. 5. Satisfactory fits for the K562 data were obtained, in which h and n did not change, and the boundaries for θ were approximated (Table S2). If the intracellular iron concentration detected by IRP were 100-fold that provided by Tf, cells would concentrate 100-fold externally available iron, all into the intracellular fraction detected by IRP only, before the onset of storage. This situation seems very unlikely, as it implies that ferritin is used for far higher intracellular iron concentrations than 100-times that of externally provided Tf, i.e. in the μM range in our experiments. It thus seems more realistic to limit this multiplicative factor to values way lower than 100. Of note, growth resumption of progenitors from cord blood (see below) and of both KG1 and HeLa cells occurred at lower Tf concentrations than for K562 cells, indicating even lower iron needs in these cases. From this analysis it may be concluded that the concentration of intracellular, easily mobilized, and Tf-derived iron most probably falls well below a few hundred nM to support cellular division.

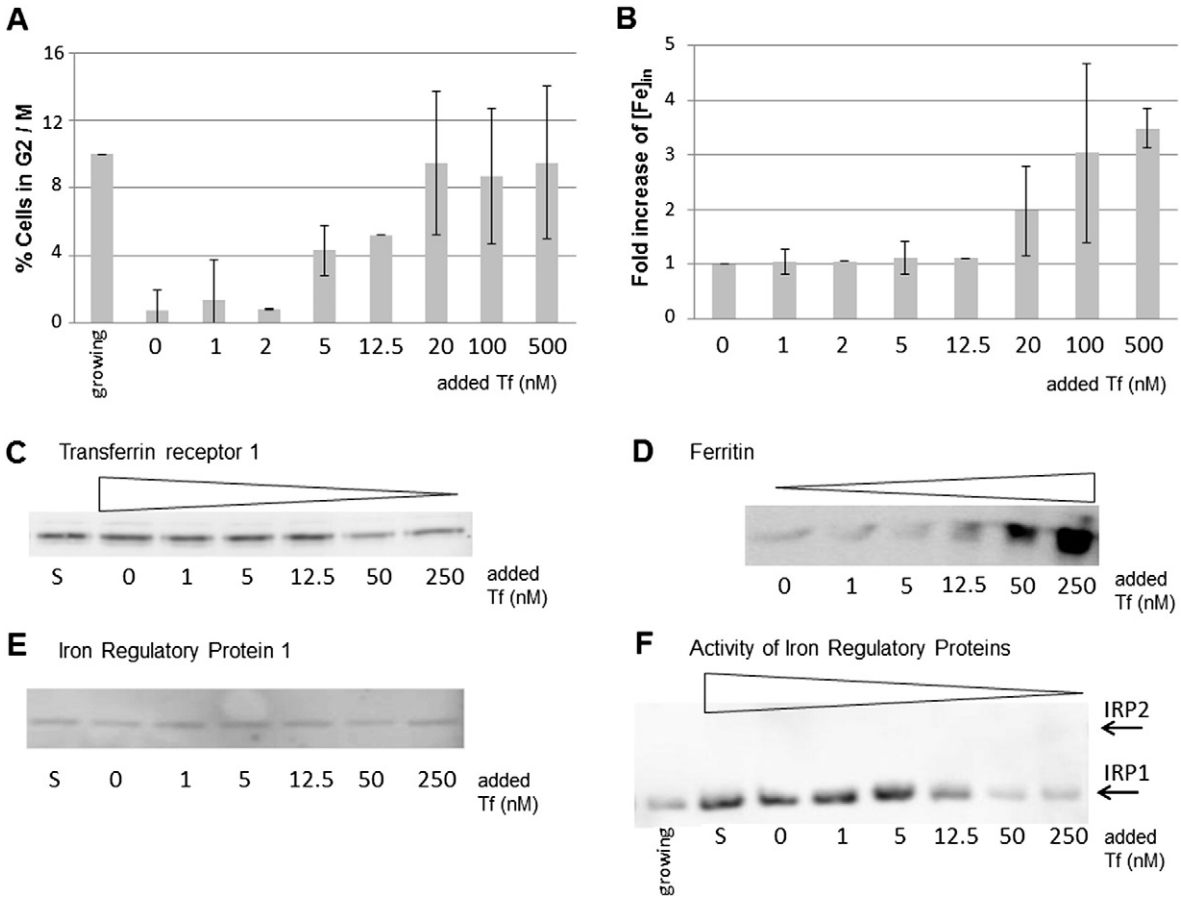

Fig. 3. Recovery of iron-depleted K562 cells after addition of holo-transferrin. (A) Re-entry in the cell cycle after 24 h of replenishment with iron-loaded Tf (Tf), as measured in different experiments (N = 3) by integration of the G2/M peak. (B) Fold increase of the iron amount associated with the cells (N = 3). The average amount of Fe is 60 pmol/10^6 K562 cells in the absence of Tf (Tf = 0). (C–E) Western blots of one representative experiment showing Tf receptor 1, ferritin, and IRP1, respectively, as a function of added Tf to iron depleted cells. S is the sample taken at the end of iron depletion, i.e. 24 h before the other iron-rescued samples. (F) RNA electrophoretic mobility shift assay of lysates from iron replenished cells with the indicated Tf concentrations in the same experiment. The positions of the shifted bands corresponding to recombinant IRP1 and IRP2 (see Fig. S2) in this assay are indicated on the right side. Triangles are included to indicate the direction of significant changes, but they do not imply monotonous variations.

3.5. Transferrin dependence for amplification of CD34$^+$ progenitors

CD34$^+$ progenitors were isolated from cord blood and the influence of Tf-bound iron on growth was studied for comparison with cell lines. The purification procedure gave preparations with more than 80% (mean 89.2% SD 5.3 for 13 experiments) of quiescent CD34$^+$ cells (Fig. 6A).

To circumvent the uncertainties in the composition of the complex media supporting culture of CD34$^+$ cells, a minimal medium of well-defined composition (see Section 2.5) was designed following the pioneering work of others [20]. The purified progenitors proliferated in the medium containing *ca.* 1 μM holo-Tf, with up to a 4-fold increase of CD34$^+$ cells after 3 days. Accordingly, the proportion of cells in the G2/M phase meanwhile rose (Fig. 6B) from 0 after isolation to up to 8%. Amplified cells could be kept for up to 9 days in culture, even with nM concentrations of Tf, and with medium changes every 3 days. Omission of Tf rapidly led to cell death without amplification or differentiation. Expansion of CD34$^+$ cells was accompanied by the increase of the cell-associated iron concentration above 200–250 nM of added Tf, but not below.

Treatment of amplified CD34$^+$ cells with up to 200 μM DFO for 24 h stopped growth (Fig. 6C), and removal of the chelator without Tf addition did not maintain viable cells (Fig. 6D). Thus, DFO-treated CD34$^+$ cells are deficient in readily available iron. But addition of holo-Tf concentrations as low as 5 nM maintained viable CD34$^+$ cells and growth resumed, as shown in Fig. 6E at 15 nM. The ferritin protein also increased with large iron provision, with a mirroring decay of Tf receptor 1 (Fig. 6F), as observed with cell lines (Fig. 3, Fig.S2). In experiments in which small concentrations of either holo-Tf (e.g. Fig. 6E) or apo-Tf (e.g. Fig. 4A) were added to the growth medium of progenitors, viability stayed at the same level with both forms of Tf for a short time (<2 days). Efforts to deplete serum albumin of bound cations (see Section 2.4) left 300 nM of iron on average (SD = 75, 7 independent measurements) in the complete minimal growth medium. Therefore, *ca.* 10 times more iron than provided by holo-Tf is present in the growth medium, and any form of Tf (apo- or recycling holo-) is needed to make a little part of non-Tf bound iron available to the cells. Yet, amplification of CD34$^+$ cells increased with added holo-Tf, indicating that iron associated with Tf turnover was the limiting factor for progression of the cell cycle. Congruent with the observations made with cell lines (Fig. 3; Fig. 4; Fig. S2), it can be concluded that CD34$^+$ progenitors enter the cell cycle and start proliferating with less than 15 nM Tf, a concentration similar to that supporting growth of KG1 and HeLa cells after DFO chelation.

4. Discussion

The present studies provide an unprecedented opportunity to estimate the amount of iron needed to support growth of hematopoietic progenitors and of different cell lines after sufficient depletion for

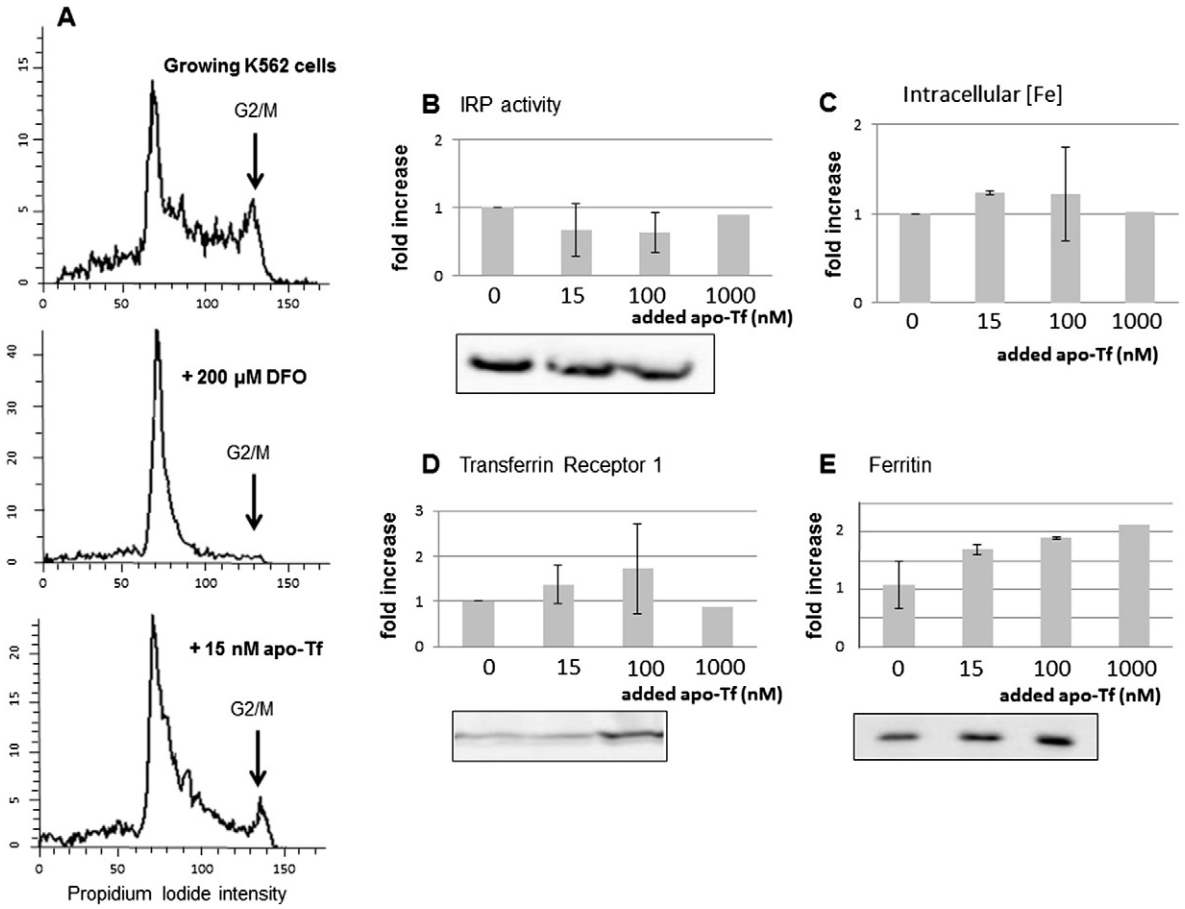

Fig. 4. Evolution of iron-depleted K562 cells after addition of apo-transferrin. (A) Cell cycle analysis of K562 cells, top: under standard (iron replete) conditions; middle: after iron removal by 200 μM DFO for 24 h; bottom: after adding 15 nM apo-Tf for 24 h to DFO-treated K562 cells. (B) IRP activity as a function of added apo-Tf. The histogram of shifted IRP-Iron Responsive Element bands is the cumulative data in which the intensity of these bands is related to the amount of IRP protein determined by Western blot and set to 1 for Tf = 0. The shifted bands of a representative experiment are shown below the relevant Tf values. (C) Iron associated with iron-depleted K562 cells after adding the indicated concentrations of apo-Tf for 24 h. The average amount of Fe is 90 pmol/10^6 K562 cells without iron addition (ApoTf = 0). (D) Tf receptor 1 and (E) Ferritin Western blots and cumulative amounts of the proteins relative to β-actin in different experiments.

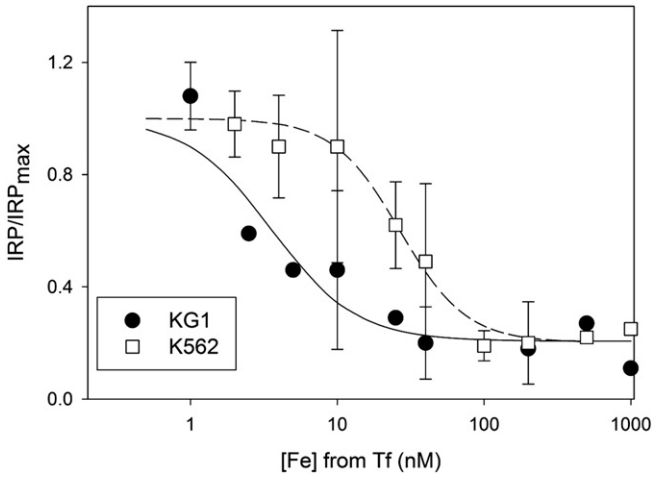

Fig. 5. Iron Regulatory Proteins sensitivity to iron-bound transferrin. The IRP activity at any given concentration of added Tf was plotted relative to that without Tf, and the drawn lines were adjusted to the experimental data with the analytical expression and the parameters reported in the text. Cumulative data from 3 different experiments for each cell line were used for this analysis, but the points without standard deviation bars were not present in all experiments.

growth arrest. A key feature of these experiments is that no external compound, such as a fluorescent probe, was added to secure readouts. Instead, a set of iron-sensitive endogenous parameters were measured to monitor levels of functional cellular iron. Accordingly, cellular stores were monitored by ferritin levels, and the amount of iron needed to reinitiate growth was precisely measured by quantitatively following the iron trafficking proteins, such as Tf receptor 1, and the activity of the cellular iron regulatory system (Iron Regulatory Proteins). The remaining iron traces in the different conditions have been taken into account by demonstrating the mandatory addition of iron-loaded Tf for proportional growth, and by showing the very limited ability of apo-Tf to mobilize residual non-Tf bound iron.

4.1. Significance of functional intra-cellular iron concentration (FIC)

The estimate of the iron amount needed to support cellular growth (Figs. 3, 5, S2) is significantly smaller than previous phenomenological measurements of exchangeable iron by fluorescent probes e.g. [21,22]. In a situation as complex as that afforded by cellular iron homeostasis, it is difficult to exactly know which iron species are detected by fluorescent molecules [23]. In contrast, the present experiments only monitor endogenous systems. Hence, the two approaches certainly have their own merits and they should be used accordingly. To acknowledge this difference, and considering the largely accepted term of *labile iron pool* (LIP) coined to the metal that can be bound by fluorescent reporter-molecules, we propose to designate by *functional iron concentration*

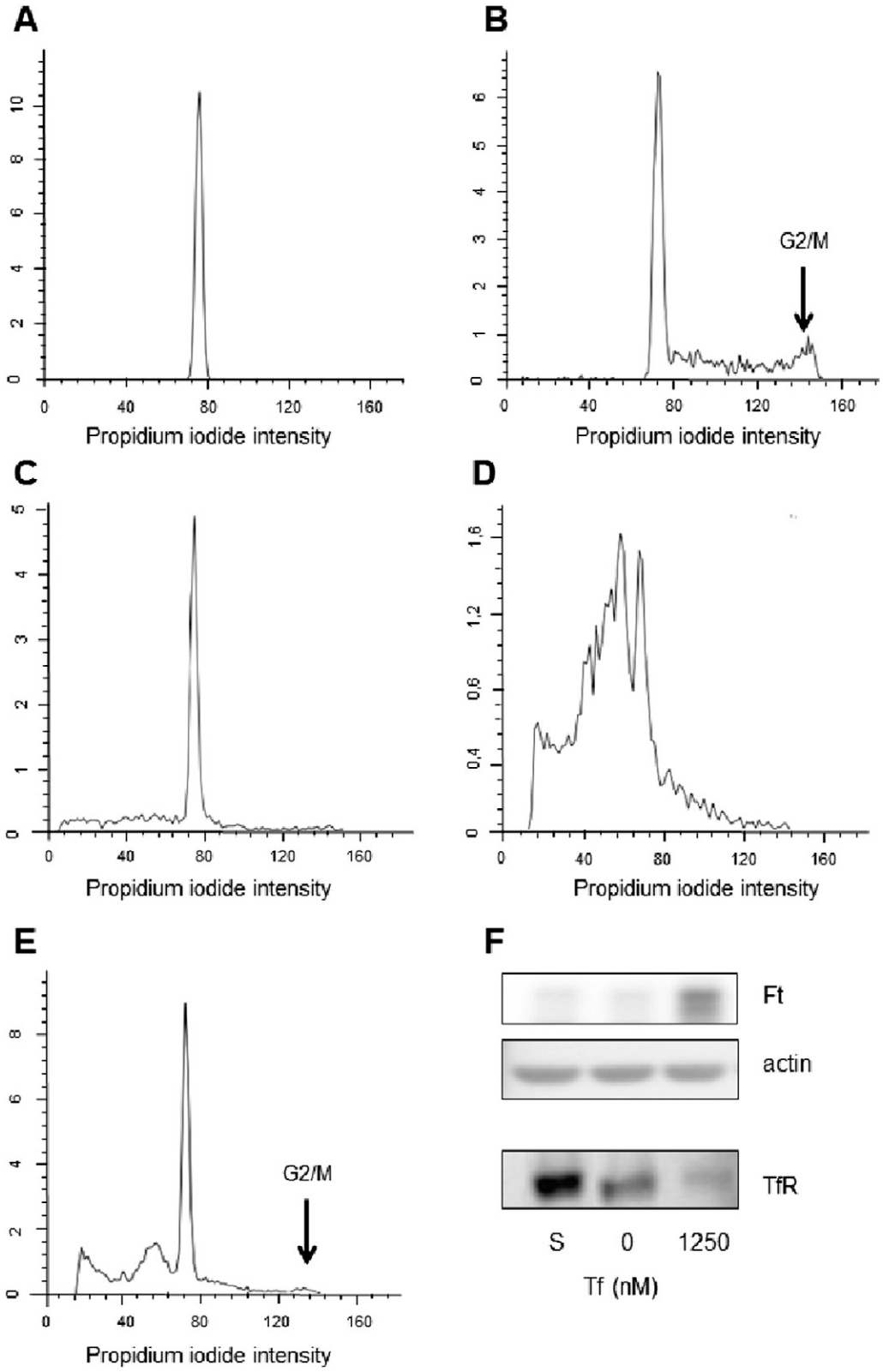

Fig. 6. Amplification of primary CD34$^+$ cells. Cell cycle analysis of CD34$^+$ cells (A) after isolation, (B) after 3 days of amplification in the complete medium, (C) as in (B) and an additional day in the presence of 200 μM DFO, (D) as in (C) and an additional day in the complete medium without Tf, (E) as in (C) and an additional day in the complete medium with 15 nM Tf. (F) Isolated CD34$^+$ cells were amplified for 3 days, treated with 200 μM DFO for 24 h (S), and kept for an additional day in the minimal synthetic medium supplemented with 1.25 μM Tf or not (0). The indicated proteins were detected by immuno-blotting.

(FIC) that detected by the endogenous iron-responsive systems, mobilized for viability, and estimated here. Increases of the LIP have often been proposed to participate to increased oxidative stress via intracellular Fenton-like chemistry, whereas the FIC identified herein does not generate any sign of oxidative imbalance (Table S1).

The lower values of FIC as compared to LIP brings the available intracellular iron concentration closer to those of other essential transition metals, including zinc which is generally found in total amounts similar to those of iron in biological systems. Indeed, despite the relatively large quantities of zinc present in cells (>μM), the cytosolic concentration of the Zn^{2+} ions is buffered largely below nM values [24]. In the case of iron the θ values of the FIC fall below the dissociation constants measured for most iron-containing enzymes and proteins [25]. Without entering into a thorough discussion of this point, it is of note that the only iron chaperones postulated in mammalian cells belong to the poly(rC) binding proteins (PCBP) family [26]. The lowest dissociation constant describing the binding of the first iron atom to PCBP1 is below 1 μM [27], and the transfer of that iron to ferritin, the first proposed substrate of iron loaded PCBP1/2, displays thermodynamic constants in the 0.2–0.3 μM range. These data perfectly fit in the scenario emerging from our studies: the determined FIC is relevant under iron-limiting conditions, before the involvement of PCBP and the need for storage in ferritin. Thus, the idea of a FIC adds a missing link in mammalian cellular iron homeostasis by depicting the available iron readily delivered by Tf for immediate cellular needs, i.e. below the iron concentrations demanding storage.

4.2. Consequences for normal and pathological hematopoiesis, and other conditions

The observations and quantitative evaluations made with the K562 and KG1 cell lines also apply to the primary cells they can be considered to derive from. Amplification of the $CD34^+$ cord blood progenitors was efficient in minimal medium (Fig. 6B) with small, in the nM range, concentrations of Tf. The low FIC values are of relevance in pathological situations. For instance, myelodysplastic syndrome (MDS) patients often need regular transfusions to reach a suitable circulating hemoglobin concentration. However, this treatment is prone to induce iron overload and a majority of these patients benefit from iron chelation therapy in terms of overall survival [28] and dependence on transfusion. Acute myeloid leukemia (AML) as cause of death in non-refractory anemia with ring sideroblasts MDS patients was annihilated by iron chelation in a retrospective clinical analysis [29]. Hence, the AML clones likely grew on the ample iron provision afforded by transfusions, and the continuing presence of chelator counteracted this effect. Iron manipulation to oppose growth of cancer cells should thus integrate the presently determined concentrations as target values to optimize efficiency while minimizing risks. Another example is the widespread provision of erythropoietic stimulating agents (ESA) in cancer related, radiation- or chemotherapy-induced, anemia. Patients suffering from cancer related anemia with low Tf saturation and medium/low ferritin may be offered a combination of ESA and intravenous iron under various forms (dextran, sucrose, gluconate, etc.) in a relatively short period of time [30]. Increased hemoglobin levels and decreased needs for transfusions are efficiently reached in clinical studies [30], often with increase of the Tf saturation (and of circulating ferritin) in responding patients with very low (<20%) values before enrollment. But the still incomplete evaluation of intravenous iron injections, particularly in the long run, is requested [30].

5. Conclusions

The requirement for proper iron monitoring, especially in a clinical context, is called for by our studies, which show that even low Tf concentrations and small iron loads, at low nM levels, promote growth of transformed cells. Such cells may remain after or during chemotherapy, hence increasing the risk of relapse with sustained iron provision. Iron chelation [31] and iron deprivation with drug delivery by targeting Tf receptor 1 [32] afford high hopes in anti-cancer therapies. With the presently reported information at hand, this promising field should focus on the differences between iron homeostasis in normal and pathological cells [33] in order to allow design of more targeted and efficient treatments.

Competing Interests

The authors declare that they have no competing interests

Transparency document

The Transparency document associated with this article can be found, in the online version.

Acknowledgements

Cécile Cottet-Rousselle and David Laurin are thanked for their valuable help with the flow cytometry instrument belonging to the LBFA technical facility and purification of hematopoietic progenitors, respectively.

This work was supported by grants from *Région Rhône-Alpes* (Programme Cible 2010), *Institut Rhône-Alpin des systèmes complexes* (IXXI), *Université Joseph Fourier Grenoble* (Programme Agir 2013), *Direction de la Recherche Clinique* (DRC) CHU Grenoble, and Novartis. The company played no role in the design and the interpretation of the results. EP is the recipient of a grant from the *Société Française d'Hématologie* (SFH).

Appendix A

The temporal evolution of active IRP has been previously described [19] and it has the following form:

$$\frac{dy}{dt} = k_1 - k.\sigma.y - k_2\,.y$$

where y is the variable representing the concentration of active IRP, k_1, k, and k_2 are the kinetic constants for non-regulated production, iron-dependent inactivation, and non-regulated degradation of IRP, respectively. σ is a sigmoid function of available iron ([Fe]) and of the iron threshold (θ) regulating the IRP activity according to:

$$\sigma = [\mathrm{Fe}]^n / ([\mathrm{Fe}]^n + \theta^n)$$

in which n represents the steepness of the iron regulation of IRP. Under conditions of extreme iron shortage, as implemented after iron chelation and growth arrest with onset of cell death, σ ~ 0, and, assuming that the IRP activity has reached a stationary state ($dy/dt = 0$), $y = y_{\max} = k_1/k_2$.

After 24 h of iron replenishment, it is assumed that cells have reached a density dependent on the externally provided iron (bound to transferrin). This density does not increase further and it corresponds to a steady state. This assumption appears valid for small transferrin concentrations, since proliferation is not supported beyond this time limit and cell death starts in the absence of further iron addition. At higher iron concentrations it is less correct as growth continues for a number of divisions which parallels iron provision. The steady state assumption ($dy/dt = 0$) implies:

$$\frac{y}{y_{max}} = \frac{k_1}{k\sigma + k_2} \times \frac{k_2}{k_1} = \frac{k_2}{k\sigma + k_2} = {}^{1}\Big/\left(\frac{k\sigma}{k_2} + 1\right)$$

writing $h = k/k_2$ and developing:

$$\frac{y}{y_{max}} = \frac{[\mathrm{Fe}]^n + \theta^n}{h[\mathrm{Fe}]^n + [\mathrm{Fe}]^n + \theta^n} = \frac{[\mathrm{Fe}]^n + \theta^n}{(h+1)[\mathrm{Fe}]^n + \theta^n}$$

which is Eq. (1) used in Fig. 5.

Appendix B. Supplementary data

Supplementary data to this article can be found online at http://dx.doi.org/10.1016/j.bbamcr.2015.03.009.

References

[1] N.T. Le, D.R. Richardson, The role of iron in cell cycle progression and the proliferation of neoplastic cells, Biochim. Biophys. Acta 1603 (2002) 31–46.
[2] J.A. Cotruvo, J. Stubbe, Class I ribonucleotide reductases: metallocofactor assembly and repair in vitro and in vivo, Annu. Rev. Biochem. 80 (2011) 733–767.
[3] A.M. Merlot, D.S. Kalinowski, D.R. Richardson, Novel chelators for cancer treatment: where are we now? Antioxid. Redox Signal. 18 (2013) 973–1006.
[4] E. McLean, M. Cogswell, I. Egli, D. Wojdyla, B. de Benoist, Worldwide prevalence of anaemia, WHO Vitamin and Mineral Nutrition Information System, 1993–2005, Public Health Nutr. 12 (2009) 444–454.
[5] WHO, Micronutrient Deficiencies, 2014.
[6] L.I. Zon, Intrinsic and extrinsic control of haematopoietic stem-cell self-renewal, Nature 453 (2008) 306–313.
[7] Y. Ginzburg, S. Rivella, Beta-thalassemia: a model for elucidating the dynamic regulation of ineffective erythropoiesis and iron metabolism, Blood 118 (2011) 4321–4330.
[8] N. Shenoy, N. Vallumsetla, E. Rachmilewitz, A. Verma, Y. Ginzburg, Impact of iron overload and potential benefit from iron chelation in low-risk myelodysplastic syndrome, Blood 124 (2014) 873–881.
[9] C. Callens, S. Coulon, J. Naudin, I. Radford-Weiss, N. Boissel, E. Raffoux, P.H. Wang, S. Agarwal, H. Tamouza, E. Paubelle, V. Asnafi, J.A. Ribeil, P. Dessen, D. Canioni, O. Chandesris, M.T. Rubio, C. Beaumont, M. Benhamou, H. Dombret, E. Macintyre, R.C. Monteiro, I.C. Moura, O. Hermine, Targeting iron homeostasis induces cellular differentiation and synergizes with differentiating agents in acute myeloid leukemia, J. Exp. Med. 207 (2010) 731–750.
[10] E. Paubelle, F. Zylbersztejn, S. Alkhaeir, F. Suarez, C. Callens, M. Dussiot, F. Isnard, M.T. Rubio, G. Damaj, N.C. Gorin, J.P. Marolleau, R.C. Monteiro, I.C. Moura, O. Hermine, Deferasirox and vitamin d improves overall survival in elderly patients with acute myeloid leukemia after demethylating agents failure, PLoS ONE 8 (2013) e65998.
[11] M. Roth, B. Will, G. Simkin, S. Narayanagari, L. Barreyro, B. Bartholdy, R. Tamari, C.S. Mitsiades, A. Verma, U. Steidl, Eltrombopag inhibits the proliferation of leukemia cells via reduction of intracellular iron and induction of differentiation, Blood 120 (2012) 386–394.
[12] X. Brazzolotto, J. Gaillard, K. Pantopoulos, M.W. Hentze, J.M. Moulis, Human cytoplasmic aconitase (Iron regulatory protein 1) is converted into its [3Fe–4S] form by hydrogen peroxide in vitro but is not activated for iron-responsive element binding, J. Biol. Chem. 274 (1999) 21625–21630.
[13] C. Dycke, C. Bougault, J. Gaillard, J.P. Andrieu, K. Pantopoulos, J.M. Moulis, Human iron regulatory protein 2 is easily cleaved in its specific domain: consequences for the haem binding properties of the protein, Biochem. J. 408 (2007) 429–439.
[14] D.B. Lipka, M.C. Wagner, M. Dziadosz, T. Schnoder, F. Heidel, M. Schemionek, J.V. Melo, T. Kindler, C. Muller-Tidow, S. Koschmieder, T. Fischer, Intracellular retention of ABL kinase inhibitors determines commitment to apoptosis in CML cells, PLoS ONE 7 (2012) e40853.
[15] A. Martelli, J.M. Moulis, Zinc and cadmium specifically interfere with RNA-binding activity of human iron regulatory protein 1, J. Inorg. Biochem. 98 (2004) 1413–1420.
[16] P. Ponka, C.N. Lok, The transferrin receptor: role in health and disease, Int. J. Biochem. Cell Biol. 31 (1999) 1111–1137.
[17] E.A. Leibold, H.N. Munro, Cytoplasmic protein binds in vitro to a highly conserved sequence in the 5′ untranslated region of ferritin heavy- and light-subunit mRNAs, Proc. Natl. Acad. Sci. U. S. A. 85 (1988) 2171–2175.
[18] T.A. Rouault, M.W. Hentze, S.W. Caughman, J.B. Harford, R.D. Klausner, Binding of a cytosolic protein to the iron-responsive element of human ferritin messenger RNA, Science 241 (1988) 1207–1210.
[19] N. Mobilia, A. Donzé, J.-M. Moulis, E. Fanchon, A Model of the Cellular Iron Homeostasis Network Using Semi-Formal Methods for Parameter Space Exploration, EPTCS 92 (2012) 42–57.
[20] L.J. Murray, J.C. Young, L.J. Osborne, K.M. Luens, R. Scollay, B.L. Hill, Thrombopoietin, flt3, and kit ligands together suppress apoptosis of human mobilized CD34+ cells and recruit primitive CD34+ Thy-1+ cells into rapid division, Exp. Hematol. 27 (1999) 1019–1028.
[21] O. Kakhlon, Z.I. Cabantchik, The labile iron pool: characterization, measurement, and participation in cellular processes(1), Free Radic. Biol. Med. 33 (2002) 1037–1046.
[22] F. Petrat, H. de Groot, R. Sustmann, U. Rauen, The chelatable iron pool in living cells: a methodically defined quantity, Biol. Chem. 383 (2002) 489–502.
[23] K.P. Carter, A.M. Young, A.E. Palmer, Fluorescent sensors for measuring metal ions in living systems, Chem. Rev. 114 (2014) 4564–4601.
[24] W. Maret, Metals on the move: zinc ions in cellular regulation and in the coordination dynamics of zinc proteins, Biometals 24 (2011) 411–418.
[25] R.C. Hider, X. Kong, Iron speciation in the cytosol: an overview, Dalton Trans. 42 (2013) 3220–3229.
[26] S. Leidgens, K.Z. Bullough, H. Shi, F. Li, M. Shakoury-Elizeh, T. Yabe, P. Subramanian, E. Hsu, N. Natarajan, A. Nandal, T.L. Stemmler, C.C. Philpott, Each member of the poly-r(C)-binding protein 1 (PCBP) family exhibits iron chaperone activity toward ferritin, J. Biol. Chem. 288 (2013) 17791–17802.
[27] H. Shi, K.Z. Bencze, T.L. Stemmler, C.C. Philpott, A cytosolic iron chaperone that delivers iron to ferritin, Science 320 (2008) 1207–1210.
[28] R.M. Lyons, B.J. Marek, C. Paley, J. Esposito, L. Garbo, N. DiBella, G. Garcia-Manero, Comparison of 24-month outcomes in chelated and non-chelated lower-risk patients with myelodysplastic syndromes in a prospective registry, Leuk. Res. 38 (2014) 149–154.
[29] H.A. Leitch, C. Chan, C.S. Leger, L.M. Foltz, K.M. Ramadan, L.M. Vickars, Improved survival with iron chelation therapy for red blood cell transfusion dependent lower IPSS risk MDS may be more significant in patients with a non-RARS diagnosis, Leuk. Res. 36 (2012) 1380–1386.
[30] J.A. Gilreath, D.D. Stenehjem, G.M. Rodgers, Diagnosis and treatment of cancer-related anemia, Am. J. Hematol. 89 (2014) 203–212.
[31] R.C. Hider, X. Kong, Iron: effect of overload and deficiency, Met. Ions Life Sci. 13 (2013) 229–294.
[32] T.R. Daniels, E. Bernabeu, J.A. Rodriguez, S. Patel, M. Kozman, D.A. Chiappetta, E. Holler, J.Y. Ljubimova, G. Helguera, M.L. Penichet, The transferrin receptor and the targeted delivery of therapeutic agents against cancer, Biochim. Biophys. Acta 1820 (2012) 291–317.
[33] S.V. Torti, F.M. Torti, Iron and cancer: more ore to be mined, Nat. Rev. Cancer 13 (2013) 342–355.